IEEE Access
Multidisciplinary | Rapid Review | Open Access Journal

Received February 20, 2018, accepted March 16, 2018, date of publication March 20, 2018, date of current version May 2, 2018.

Digital Object Identifier 10.1109/ACCESS.2018.2817508

Research on a Dynamic Virus Propagation Model to Improve Smart Campus Security

LEI WANG[1], CHANGHUA YAO[1], YUQI YANG[1,2], AND XIAOHAN YU[3]

[1]College of Communication Engineering, Army Engineering University of PLA, Nanjing 210007, China
[2]PLA Troop 92146, Zhanjiang 254000, China
[3]College of Command Information Systems, Army Engineering University of PLA, Nanjing 210007, China

Corresponding author: Changhua Yao (ych2347@163.com)

This work was supported by the National Natural Science Foundation of China under Grant 61702543 and Grant 71501186.

ABSTRACT This paper focuses on the security and robustness of smart campuses by studying a virus propagation model. Establishing a model that reflects the epidemiological transmission mechanism is a primary method for studying disease outbreaks and control. However, the relationship between microscopic and macrodynamic evolution in networks has long remained an unsolved problem. The existing virus transmission models, which ignore differences between individuals, cannot objectively reflect the spread of infectious diseases. In this paper, a differential model of virus propagation is established for a smart campus network by considering the differences among individuals, and a method to extend the individual evolution process to the evolution process of the entire network is proposed. First, the functional process of a virus infection in individuals is reflected by the evolution model of a single node. Then, we extend the individual evolution to the whole network to reflect the scale of virus transmission and propagation among individuals in a smart campus network. The proposed model more objectively reflects viral infections and could serve to enhance the security and robustness of smart campuses.

INDEX TERMS Smart campus, security, robustness, dynamic evolution, virus propagation.

I. INTRODUCTION

Smart campuses have recently become a hot research topic because the campus network is a basic facility. Smart campuses must be supported by fast, strong and safe campus networks. However, campus networks may be threatened by different types of viruses that could negatively impact the security of the smart campuses. To improve the security and the robustness of a smart campus network, it is important to analyze how a virus could propagate through the network. Knowledge of such propagation can improve the security and robustness of smart campuses.

Creating mathematical models of virus propagation has always been a hot topic in academia, industry, and government [1]. Scholars proposed the first mathematical frameworks of epidemic transmission as early as 1927. Two classical models that describe the propagation process of biological viruses in social networks are SIS and SIR [2], [3]. These models provide the high-level trend of virus transmission in a population, and they have remained dominant for a long time. As the SIR model shows, for all viruses to which a population can develop immunity (which provides protection from future virus outbreaks), the entire population tends to become immune [4]. Under repeated viral attacks, the SIS model shows that, in theory, a dynamic balance will eventually be struck between the number of people in the population and the health of the population. The SIS and SIR classical models are still in use and have undergone additional development. Based on these two models, the SI model, which models the early stage of a disease outbreak, and the SIRS model, which models the immune period, provide results closer to the spread of real-world viruses [5]–[7]. Some important related studies exist. Wei *et al.* [8] proposed a gradient-driven parking navigation using a continuous information potential field based on a wireless sensor network, and in [9], a modified repetitive learning control approach was proposed. In [10], Yang *et al.* studied optimum surface roughness prediction, and Cui and Qin [11] conduced virtual reality research. In [12], nonlinear dynamics and anti-sway tracking control were proposed. With the rise of network science, virus propagation model establishment is no longer isolated from the analysis of network properties. In addition, such models can also consider interactions between the networks. Thus, using network science research methods to study transmission of disease-causing and computer viruses in a network has

become a new topic. The model of virus propagation based on cellular automata shifted the attention from the overall transmission situation to one of state evolution, starting with a single individual and developing through coupling relationships. In recent years, with the continuous development of network science and network dynamics, the cellular automata model [13], [14] and coupled map lattice (CML) model can reflect changes in information transmission in the network resulting from coupling relationships between network nodes (a virus can be regarded as a special type of information), and reflect how the network state changes over time.

However, these models are also based on the assumption that nodes do not differ in behavior. Thus, these models ignore the influences of individual behaviors on the final state of the network. In addition, in fact, the influence of individual behavior on the eventual overall state of the network is both objective and even critical, because it considers such aspects as immune system differences among organisms and different congestion control strategies in the computer network, which should not be ignored.

By establishing a node behavior model that reflects the different coping mechanisms of individual network nodes, we can obtain a structure that reflects the viral evolution in an individual in each period. At the same time, based on the network communication model, the individual information is exchanged, and a method of describing the whole network from a macro perspective can be achieved.

Through comparative experiments, we found that the new model not only achieves the same results as SIS and SIR model when describing the evolution trend of the whole network but also yields the state of any single point in real time, which can help with controlling the spread of disease (or information). Simultaneously, due to differences in individual coping mechanisms, an individual early warning threshold can be set to control the spread of disease. This threshold also provides an index that can reveal individuals who need special attention.

The rest of this paper is organized as follows. In Section II, we introduce the related work. Section III presents an evolutionary model of virus propagation based on the predator model. Section IV presents a simulation of network failure propagation. Finally, conclusions are drawn in Section V.

II. RELATED WORKS ON VIRUS TRANSMISSION MODELS

Research on viral transmission models includes many classical methods. The purpose of such models is to simulate viral spread realistically. By better reflecting the mechanisms through which viruses spread, these models provide a better theoretical basis for prevention, which is the goal of virus control.

A. MEAN FIELD METHOD

The mean field method is the most concise method and the most widely used in epidemic disease the analysis [15]. This method addresses environmental effects on the object collectively by computing the average effect instead of the effects of single superpositions [16]. The SIR model hypothesis assumes that the propagation period of an epidemic is much shorter than the lifetime of an individual, which means that the death of any single individual can be ignored. The evolution process of nodes in the network is susceptible, infected, and recovered ($S \rightarrow I \rightarrow R$). However, when the propagation process completes, there are only two states: S and R.

After considering the relevant effects in the network, the SIR model that acts on the average network can be written as follows [17]:

$$\begin{cases} \dfrac{dS(t)}{dt} = -S(t)\lambda < k > I(t) \\ \dfrac{dI(t)}{dt} = -\mu I(t) + S(t)\lambda < k > I(t) \\ \dfrac{dR(t)}{dt} = \mu I(t) \\ 1 = S(t) + R(t) + I(t). \end{cases} \tag{1}$$

Here, $S(t)$, $I(t)$ and $R(t)$ indicate the node density in the three states, S, I and R, respectively, $< k >$ represents the average degree of the network, λ is the probability of disease, and μ is the probability of recovery.

To accurately describe propagation process of an epidemic in heterogeneous networks, Pastor and Vespignani proposed the heterogeneous average field method [17], [18].The differential model of the concrete SIR model is as follows [19]:

$$\begin{cases} \dfrac{dS_k(t)}{dt} = -S_k(t)\lambda k\Theta(t) \\ \dfrac{dI_k(t)}{dt} = -\mu I_k(t) + S_k(t)\lambda k\Theta(t) \\ \dfrac{dR_k(t)}{dt} = \mu I_k(t) \\ 1 = S_k(t) + R_k(t) + I_k(t). \end{cases} \tag{2}$$

The gap between model (2) and model (1) occurs mainly because of the introduction of $\Theta(t)$, which expresses the effects of different degrees on the propagation. Introducing this variable more accurately describes the probability that an edge of a given node of k is connected to an infected node:

$$\Theta(t) = \sum_{k'} P(k'|k) I_{k'}(t). \tag{3}$$

The mean field theory is widely used in the threshold of epidemic spread and in the final analysis of infection density. It also plays a dominant role in the analysis of the density of infection during homeostasis. However, the error of the mean method is also obvious: it ignores the dynamic correlations between the nodes when solving models (1) and (2). A more accurate description of the evolution of the epidemic in the network cannot assume the independence of dynamic interactions between nodes. An approximation method for these interactions is proposed in this paper.

B. POINT APPROXIMATION

Point approximation is used to describe simple spatial dynamics behavior by a set of differential equations [20].

Suppose that λ is the disease probability, and μ is the recovery probability. In the SIS model, the following differential model can be obtained [21]:

$$\begin{cases} \dfrac{d[S]}{dt} = -\sum_{SI} \lambda + \sum_{I} \mu \\ \dfrac{d[I]}{dt} = \sum_{SI} \lambda - \sum_{I} \mu \\ [S] + [I] = N, \end{cases} \tag{4}$$

where $[S]$ and $[I]$ indicate the number of nodes in the s and I States, respectively, N is the total number of nodes, and $[SI]$ represents the number of edges between nodes in the S state and nodes in the I state. Then, the equations of the different types of edges specific to the approximation method are expressed as follows [22]:

$$\begin{cases} \dfrac{d[SS]}{dt} = -2\sum_{SI} \lambda Q(S|SI) + 2\sum_{I} \mu Q(S|I) \\ \dfrac{d[SI]}{dt} = \sum_{SI} \lambda [Q(S|SI) - Q(I|SI)] \\ + \sum_{I} \mu [Q(I|I) - Q(S|I)] \\ \dfrac{d[II]}{dt} = 2\sum_{SI} \lambda Q(I/IS) - 2\sum_{I} \mu Q(I|I) \\ [SS] + 2[SI] + [II] = M, \end{cases} \tag{5}$$

where $Q(I|SI)$ represents the average number of I nodes in the point neighborhood of the S state from the $S - I$ edge

Point approximation is applicable to network structures without loops, and the dynamic process description of a topological multi-part-tree structure is more accurate. However, there are too many circuits in actual social networks, making this method difficult to formulate accurately.

C. THE MODELING PRINCIPLE

In dynamic models of disease spread, several types of dynamic models are typically established to make the model more realistic. However, the spread of disease in reality cannot be rigorously studied if only the interactions between nodes are studied but the differences between individuals are ignored. The immune systems of different individuals causes different outcomes between individuals infected with the same virus. At the same time, in reality, diseases also have a latent period and models must consider the evolution of the second immune system. If these individual dynamics and the overall dynamics of the network were to be combined, the theory would more closely mimic actual situations.

However, selecting an appropriate method to model individual expression of the special viral information is the main problem. Here, a property relation model method is proposed. The specific ideas are shown in the following flow chart:

From Figure 1, it is clear that using a differential equation or a difference equation to describe the relationships between each attribute can not only reflect the changes in the quantity of each attribute over time but also the differences between individuals based on the differences in the initial attribute values.

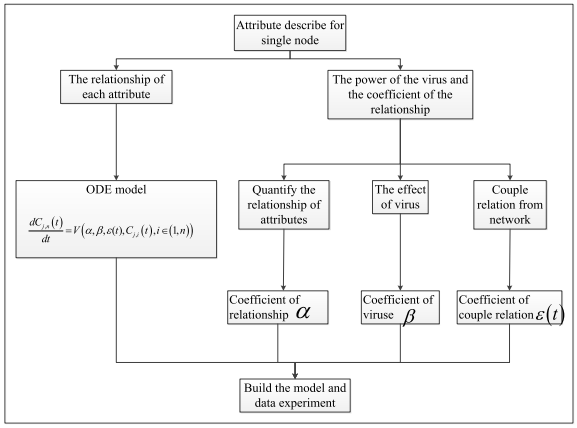

FIGURE 1. The System Model.

From the flow chart, it can be seen that the node states are no longer simple 0s and 1s as in the classical model; instead, each node state is a continuous value that can describe the individual's health degree and introduces death as a consideration during the node evolution process. Consequently, the result is more consistent with the actual situation. Moreover, it is universally important to model the attribute relationships within an individual using the principles of biological viruses. The effects of different viruses can then be simulated by modifying the virulence factors of different viruses to represent state changes over time.

III. EVOLUTIONARY MODEL OF VIRUS PROPAGATION BASED ON THE PREDATOR MODEL

A. FACTOR ATTRIBUTE OF ORGANISM

After entering an individual, the virus invades a host cell and uses the machinery and nutrients of the host cells to power a large amount of replication. Then, it breaks up the host cell, allowing the replicants to spread and infect other cells. At the same time, the immune system uses leukocyte phagocytosis and other means to eliminate these foreign invaders. The state of a given individual is defined by the vector $s = (V, C, W)$, where V represents the number of viruses in the body, C represents the number of individual host cells, and W represents the number of immune cells in the body. The states changes over time, which are represented by the function vector $s(t) = (V(t), C(t), W(t))$.

To describe an individual's health condition, the node state vector is mapped to specific quantitative indexes; the node states are then reflected through these quantitative indexes. We define F as the mapping, which represents the health of an individual as follows:

$$F(s(t)) : R^3 \mapsto [0, 1]. \tag{6}$$

Here, $F(s(t)) = 1$ represents the highest degree of a diseased node, and $F(s(t)) = 0$ represents a healthy node. A fully healthy individual is defined as one with no virus, and an individual's death occurs when all the host cells become

inactive. Based on the definition of the function vector, in a simple plane, $S_1 = \{(0, x, y), x > 0, y \geq 0\}$ expresses a completely healthy state, the line $S_2 = \{(z, 0, 0), z \geq 0\}$ expresses a dead state, and S_1 and S_2 are mutually perpendicular. The state of the whole evolution can be modeled to a first approximation within the limits of three-dimensional space. Define vector a as a health reference vector. Then Formula (6) becomes

$$F(s(t)) = 1 - \frac{\langle s(t), e\rangle}{\|s(t)\|_2 \|e\|_2} \frac{C(t)}{C(0)}. \tag{7}$$

From Formula (7) we can see that the cosine of the angle between the state vector $s(t)$ and the health reference vector e is used as the state mapping. Formula (7) shows that within a time period, the health status of an individual is expressed by the angle between the state $s(t)$ and the plane S_1 and the ratio of the number of active host cells to the initial number of active host cells. The larger the angle is, the more that individual deviates from the healthy state.

When an individual recovers after the immune cycle, the virus in that individual is eliminated. However, the number of active cells that individual has does not return to the original level; therefore, the individual's state of health is still poor. Figure 2 shows a geometrical representation of the state map.

$$F(s(t)) = 1 - \cos(\theta) \frac{C(t)}{C(0)}. \tag{8}$$

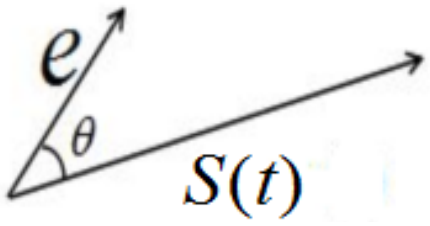

FIGURE 2. Geometric representation of state mapping.

B. ATTRIBUTE RELATIONSHIP MODEL BASED ON THE PREDATOR-PREY RELATION

The number of viruses is related to both the number of host cells and the viruses themselves. In individuals, after a virus infects a cell, it subsequently releases more viruses. Simultaneously, as the viral load increases, the immune function becomes activated, and immune cells proliferate, which inhibit the rate of viral growth. In general, the virus preys on cells, and the immune system preys on viruses.

The relationship shown in Figure 3 can be expressed in the form of a differential equation seas follows:

$$\begin{cases} \frac{dV(t)}{dt} = V(t)(aC(t) - bW(t)) \\ \frac{dC(t)}{dt} = C(t)(c - dV(t)) \\ \frac{dW(t)}{dt} = W(t)(-e + fV(t)). \end{cases} \tag{9}$$

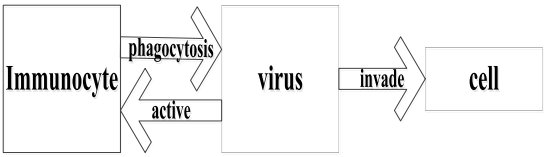

FIGURE 3. Attribute relationship factor diagram.

The change in an individual's state is reflected in comparison to the initial value. For example, the initial value $(0, c, 0)$ indicates an individual who has had no contact with the virus and therefore has no corresponding antibodies; The initial value $(v, c, 0)$ denotes an individual with no prior viral contact who is infected by the virus; The initial value (v, c, w) represents an individual with antibodies once again in contact with the virus (the secondary immune process of the organism).

The model (9) and the actual immune process are different as well; thus, we need to improve the model to make it more realistic. First, the host recovers appropriately after the disease, but is then restored to the initial value in a state of equilibrium. After a virus is eliminated, the immune cells do not remain at high numbers; they become reduced to a low (but not zero) value. Based on these conditions (9), the following models can be obtained:

$$\begin{cases} \frac{dV(t)}{dt} = V(t)(aC(t) - bW(t)) \\ \frac{dC(t)}{dt} = \frac{C(t) - sgn(C(t) - C(0))C(t)}{2} \\ \quad \times (c - dV(t)) \\ \frac{dW(t)}{dt} = W(t)(-e + fV(t)). \end{cases} \tag{10}$$

C. DETERMINATION OF MODEL PARAMETERS

In the differential equation set in Formula (10), the parameters describe the relationships among the three factors. These parameters describe the body functions and the ability of a virus to become pathogenic. In this paper, all the parameters are divided into two sets, α and β. One set is a collection of internal relations (parameter β), which include the individual's own cell renewal level $\{c, e\}$, the phagocytic ability of immune cells b, and the immune system's response capability f, namely, $\{c, e, b, f\} \in \beta$. The other is a collection of external relations (parameter α), which include the pathogenic ability of the virus d and the propagation capacity a of the virus in the body, namely, $\{a, d\} \in \alpha$. Parameter set α indicates viral differences, while coefficient set β reflects the individual functional differences. The initial value $(V(0), C(0), W(0))$ reflects the differences among individuals' initial states. The values for collection α can be determined by referring to medical experiments.

Taking the viral invasion of a human nasopharyngeal carcinoma cell line CNE as an example, the following information can be obtained from data reported in [22], which studied the effect of a virus on the nasopharyngeal carcinoma cell line CNE. The survival rate of epithelial cells exposed to the

virus was less than 60 % under normal conditions. On the other hand, the virus increased 50 times more than normal over 24 hours in the CNE environment; the cells were distributed in an observation well of $100\mu L$ with a density of $1 \times 10^5/mL$, and the virus titer MOI is 1. Based on these data from the literature, the partial coefficients of the model in (10) are set as shown in Table 1.

TABLE 1. The collection parameters.

a	0.005
d	0.4

The model coefficient set α (Table 1) and the numerical experiment using these initial values can be visualized as shown in Figure 4.

The different initial values and the numerical experiments using different values for the parameter set β are reflected in Figure 4. As shown in Figure 4(A), the establishment and description of the model is in line with the biological immune process, that is, the virus kills the cell but simultaneously stimulates the immune cells to kill the virus. Figure 4(B–D) reflects the evolution of the virus, the host cells and the immune cells derived from varying the parameter collection β to reflect different internal relationship parameters. These results also conform to the rules of immunity. As shown in Figure 4(C), the pathogenicity of the virus is sufficient to kill a large number of cells within a very short time; with no outside help, this virus would be difficult to overcome.

D. THE PLANE GRAPH OF THE MODEL AND THE ANALYSIS OF ITS SOLUTION

After analyzing the model and the coefficients, considering that model (10) is a nonlinear differential equation set, obtaining an analytical solution is difficult. Therefore, for the model proposed in this paper, the solution and analysis of the model are shown by the plane figure of the solution and the analytical method of sexual state. The parameters corresponding to those used to create Figure 4(A) are shown in Table 2.

TABLE 2. The parameters used for the model in Formula (10).

a	0.005
b	0.0005
c	1
d	0.4
e	0.3
f	0.4

Among the initially selected values, the Take interval of the virus is [30, 100] and the corresponding value of the immune cells is $W(0) = C(0)/30$.These three factors are depicted graphically in Figure 5.

Figure 5(A) shows a trend diagram of the change over time between the three factors' properties. Figure 5 (B, C, D) show the results of projecting (A) to three planes, respectively. Figure 5 (A) shows the overall evolution of the three

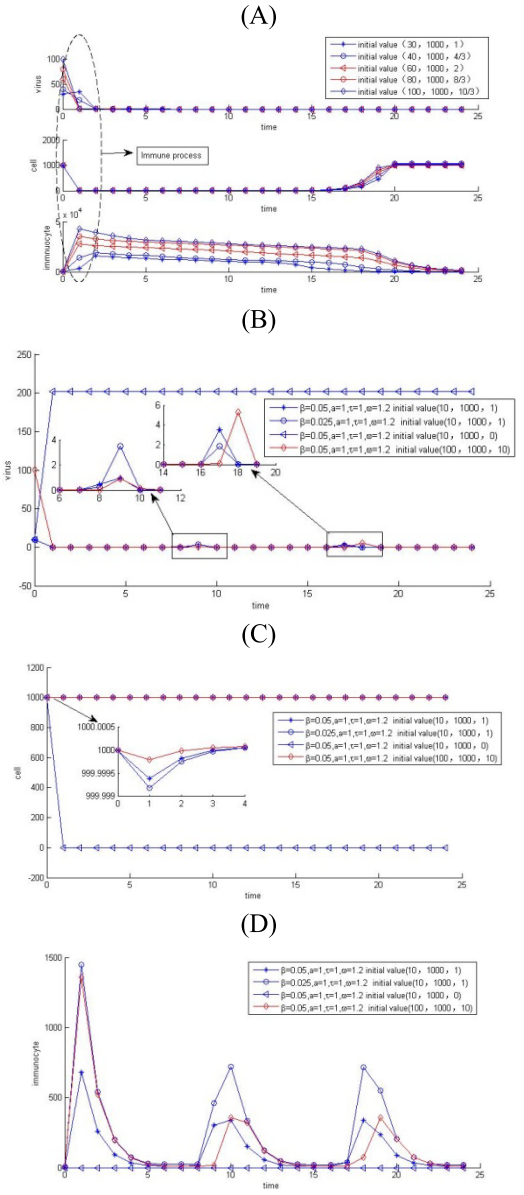

FIGURE 4. Evolutionary process map of organism properties.

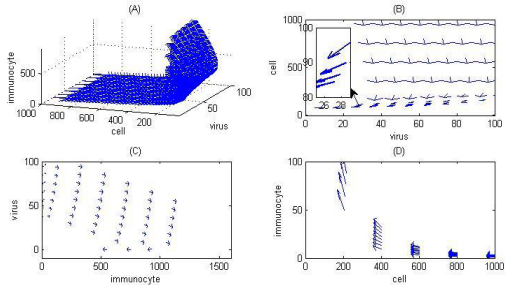

FIGURE 5. Relationships between attribute of the organism and the plane Figure.

properties (decreased number of host cells and virus load and increased immune cells). The graph in Figure 5(B) reflects the relationship between host cells and viruses, showing that in the initial disease stage, the pathogenicity causes a dramatic

increase in the number of cell deaths; however, when the number of surviving cells is less than 80, the viral effect on cells decreases with the number of viruses and becomes flat. At the same time, in Figure 5(C), the increase in the number of virus causes the number of immune cells to increase, and when the number of immune cells reach a certain level, they inhibit further increases in the amount of virus. As this plane figure shows, modeling can describe the immune process of an individual; the modeling is consistent with the actual situation.

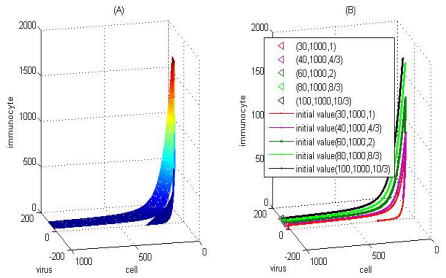

FIGURE 6. Organism immunity graph and rail lines.

Figure 6 shows a 3D graph (6(A)) and rail lines (6(B)) corresponding to different initial values. The change trends of the tracks are consistent with Figures 3–5. As seen from Figure 5 and Figure 6, all the rail lines intersect the plane at $S_1 = \{(0, x, y), 0 < x < 80, y \geq 0\}$. This shows that after a sufficiently long period, the virus will be engulfed, but the number of nodes that survive viral thinning is very low; thus, the node state represents serious illness or death.

E. CHANGES IN THE NETWORK NODE STATE

An important aspect for establishing the node evolution model is to provide equations that model the independent evolution of each node and that reflect how the state changes over time through a state function (7). Because nodes are a major part of a network structure, it is very important to study node states. By comparing the state changes of a node under different initial value conditions, we can then target approaches to protecting the nodes. Even for highly pathogenic viruses such as H1N1, improving the antiviral capacity of the individual nodes is highly significant to the evolution of the entire network.

As Figure 7 shows, improving the immune ability of an individual reduces the period during which the individual is in the diseased state. However, because of the strong pathogenicity of the virus, its sensitivity to the immune system is low.

This section describes the evolution of the three important factors of life during a viral invasion through the establishment of relational differential equations that describe the effects of separating individuals from the biological social network in the face of the evolutionary process of disease invasion. Through the relationships shown in the plane figure, by performing experiments with the virus, we find that the pathogenic ability of virus becomes extremely high under the influence of the evolution of the other nodes in the network;

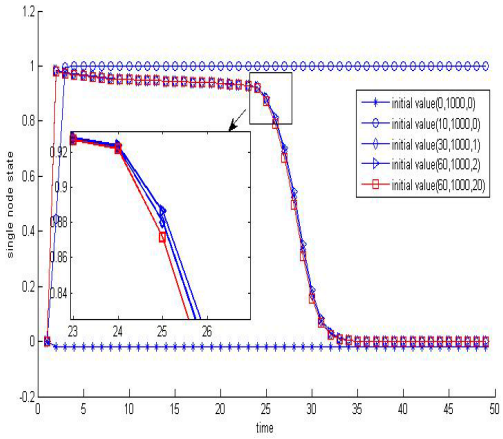

FIGURE 7. Health degree.

thus, we cannot ignore the influence of node death within the network.

IV. SIMULATION OF NETWORK FAILURE PROPAGATION

Considering the node attribute relationship model of the disease transmission network described in Section 3, the virus is transmitted through a social network, that is, the virus is the main information exchanged in this network, and viral transmission among different nodes should be considered in the evolution of the individual.

Let $s(t)_i = (V_i(t), C_i(t), W_i(t))$ represent the ith node in the network, and let θ represent the proportion of the virus exchanged during interactions. Here, A represents the adjacency matrix of the entire social network, and Formula (10) joins the node coupling relationship. Then, the ith node can be represented as follows:

$$\begin{cases} \dfrac{dV_i(t)}{dt} = V_i(t)(aC_i(t) - bW_i(t)) \\ \qquad\qquad + \displaystyle\sum_{j=1}^{n} \theta_j a_{ij} V_j(t) - \theta_i V_i(t) \\ \dfrac{dC_i(t)}{dt} = \dfrac{C_i(t) - sgn(C_i(t) - C_i(0))\, C_i(t)}{2} \\ \qquad\qquad \times (c - dV_i(t)) \\ \dfrac{dW_i(t)}{dt} = W_i(t)(-e + fV_i(t)). \end{cases} \tag{11}$$

The model in Formula (11) shows the node model after joining and coupling. As mentioned in the introduction, when the scale of the network is large, solving model is quite difficult. Therefore, this paper uses an approximate iterative method to simulate the coupling process of the network. This process involves dividing the long-term evolution of the network into a series of evolutionary cycles T_p. In each cycle, only the evolution of each individual node is considered; the influences of other nodes on the network are ignored. At the end of a cycle, the network information is exchanged, followed by the next cycle. This process is iterated until the different states of the number of nodes in the network are relatively stable, at which point the algorithm is terminated.

TABLE 3. The basic network properties.

Network type	Total nodes	Power law distribution
The social network	2,180	3.2

A. NETWORK CHARACTERISTICS AND DETERMINING THE ITERATIVE PERIOD

Networks formed by the interactions of social individuals are typically complex. Social networks include a series of relational subnetworks, such as those formed by friendship relationships and working relationships. Scholars have made great strides in research concerning large-scale social networks; these advances provide the basis for research of infectious diseases in biological networks.

According to [23] and [24], it is assumed that the nature of the communication network in this article is as shown in Table 3.

The interval from the time that an individual is infected to the time they become a viral vector is related to both the evolution of the virus itself and the individual's social contacts. The time required to exchange a virus between two individuals is the individual evolution cycle T_p. T_p is related to the status of an individual in a social network, which is expressed by the degree d_i of each individual in a social network. Thus, $T_p(d_i)$ represents the viral evolution cycle of individual i.

Based on reports from [22], set $T_p(d_i) = 24(md_i)^{-1}$, where m represents the proportion of social competence in an individual. For individuals who have a large impact on the network, the elapsed time from infection to viral exchange with other individuals is smaller than those of other, less important nodes.

B. NETWORK INTERACTIONS AND MODEL OPERATIONAL RULES

The vector function $s(t)$ represents the state of a node at point t. We define a vector function, $n(t)$, to represent the state of the whole network as follows:

$$n(t) = \begin{pmatrix} s_1(t) \\ s_2(t) \\ \vdots \\ s_n(t) \end{pmatrix} = \begin{pmatrix} V_1(t) & C_1(t) & W_1(t) \\ V_2(t) & C_2(t) & W_2(t) \\ \vdots & \vdots & \vdots \\ V_n(t) & C_n(t) & W_n(t) \end{pmatrix}. \quad (12)$$

Based on the topological structure of the network, the adjacency matrix of the network can be obtained, which is denoted as $A(t)$. Because of the need to remove ill individuals from the network, the topology of the network must be adjusted over time:

$$F(n(t)) = \begin{pmatrix} F(s_1(t)) \\ F(s_2(t)) \\ \vdots \\ F(s_3(t)) \end{pmatrix}. \quad (13)$$

Here, $F(n(t))$ represents a state metric for each node of the network. The viral propagation can then be expressed formulas follows:

$$\begin{pmatrix} V_1(t) \\ V_2(t) \\ \vdots \\ V_3(t) \end{pmatrix}^T = \begin{pmatrix} V_1(t-1) \\ V_2(t-1) \\ \vdots \\ V_3(t-1) \end{pmatrix}^T \{[F(n(t-1))] * A(t) - \varepsilon I\}. \quad (14)$$

The $*$ operation between the vector $[F(n(t-1))]$ and the matrix $A(t)$ in Formula (14) is the direct sum of the column vector $[F(n(t-1))]$ and the corresponding elements of each column of $A(t)$ (15), as shown at the bottom of this page.

Because disease outbreaks are stochastic, they can be regarded as a stochastic fault in a social network. Thus, the process of the periodic evolution model proposed in this paper is as follows:

Step 1: Attach random virus values to the nodes of the network such that some individuals contain a certain number of viruses,

Step 2: Evolve each node in the network over a cycle T_p, as described in 4.2.1;.

Step 3: Using Formula (14), conduct an exchange based on the number of individual viruses in the network. Record the nodes that substantially deviate from the health state and eliminate dead nodes.

Step 4: During the exchange, the number of individual viruses is taken as the initial value. Then, the process returns to the second step to simulate viral evolution in each node. The node evolution process based on this periodic algorithm is shown in Figure 8.

$$[F(n(t-1))] * A(t) = \begin{pmatrix} [F(s_1(t-1))]a_{11} & [F(s_1(t-1))]a_{12} & \cdots & [F(s_1(t-1))]a_{1n} \\ [F(s_2(t-1))]a_{21} & [F(s_2(t-1))]a_{22} & \cdots & [F(s_2(t-1))]a_{2n} \\ \vdots & \vdots & \ddots & \vdots \\ [F(s_n(t-1))]a_{n1} & [F(s_n(t-1))]a_{n2} & \cdots & [F(s_n(t-1))]a_{nn} \end{pmatrix}. \quad (15)$$

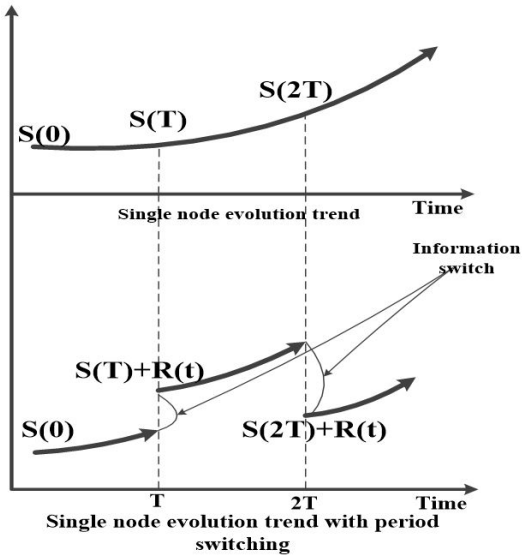

FIGURE 8. A sketch map of the node evolution process based on the proposed periodic algorithm.

C. RATIONALITY ANALYSIS THE ITERATIVE ALGORITHM

The process of the dynamic model solved by the iterative algorithm and the process described by the model in Formula (11) are similar. The main difference between the models in (10) and (11) is the network coupling. As shown in the model in (11), the coupling relationship is represented by the formula $\sum_{j=1}^{n} \theta a_{ij} V_j(t) - \theta V_i(t)$. In this relationship, $\sum_{j=1}^{n} \theta a_{ij} V_j(t)$ represents an exchange of virus between adjacent nodes, and $\theta V_i(t)$ represents the number of viruses exchanged during each process. Thus, we can divide the propagation process in (11) into two processes as follows:

$$\begin{cases} \dfrac{dV_i(t)}{dt} = V_i(t)\left(aC_i(t) - bW_i(t)\right) \\ \dfrac{dC_i(t)}{dt} = \dfrac{C_i(t) - sgn\left(C_i(t) - C_i(0)\right) C_i(t)}{2} \\ \qquad \times \left(c - dV_i(t)\right) \\ \dfrac{dW_i(t)}{dt} = W_i(t)\left(-e + fV_i(t)\right) \\ \qquad + \dfrac{dV_i(t)}{dt} = \sum_{j=1}^{n} \theta_j a_{ij} V_j(t) - \theta_i V_i(t) \\ \dfrac{dC_i(t)}{dt} = 0 \\ \dfrac{dW_i(t)}{dt} = 0. \end{cases} \tag{16}$$

The portion to the left of the plus sign denotes the evolution process, while the portion to the right of the plus sign denotes the propagation process. To signify communication, the propagation process in $V(t) = (V_1(t), \cdots, V_n(t))$, $\theta = (\theta_1, \cdots, \theta_n)$, (16) can be rewritten as:

$$\frac{dV(t)}{dt} = \theta^T V(t) A - \theta^T V(t) I \tag{17}$$

After introducing this cycle, the overall evolution model is as follows:

$$\begin{cases} \dfrac{dV(t)}{dt} = V(t)\left(aC(t) - bW(t)\right) \\ \dfrac{dC(t)}{dt} = \dfrac{C(t) - sgn(C(t) - C_i(0)) C_i(t)}{2} \\ \qquad \times \left(c - dV_i(t)\right) \\ \dfrac{dW(t)}{dt} = W(t)\left(-e + fV(t)\right) \\ \qquad + \dfrac{dV(t)}{dt} = g(t)\,\theta^T V(t) A - \theta^T V(t) I \\ \dfrac{dC(t)}{dt} = 0 \\ \dfrac{dW(t)}{dt} = 0, \end{cases} \tag{18}$$

where $g(x) = \begin{cases} 1, x = nT_p \\ 0, others \end{cases}$. When T_p becomes sufficiently small, the node evolution in Formula (18) will be approximated indefinitely (16). Therefore, the introduction of the cycle can reduce the difficulty of solving the model, and selecting a better cycle can also improve the accuracy of the operation. When $\theta_i = [F(s_i(t-1))]$, the propagation processes in (17) and (14) are equivalent.

D. NUMERICAL SOLUTION AND SIMULATION

Basic comparative data were obtained by calculating the rates of diseases (number of people/the largest number). The proposed model and the SIS model are executed using these basic data and the differences between the model results and the actual situation were evaluated.

To select the appropriate evolution cycle, by comparing the gap between the simulated data and the real data, we can reach the following conclusions:

TABLE 4. Comparison of average cycle selection effect.

Social competence score (m)	Average evolution cycle T	Proportion of final number of sick nodes	Difference from actual data (mean Euclidean distance)
1	5.58	1	7.85
2	2.77	0.97	4.74
3	1.86	0.97	4.88
4	1.41	0.96	4.14

As shown in Table 4, selecting different social ability levels affects the average evolution cycle of nodes. Selecting an average evolution cycles different from reality will result in differences between the final model and the actual data. As the social ability level increases, the evolution cycle decreases according to $T_p(d_i) = 24(md_i)^{-1}$. A decrease in

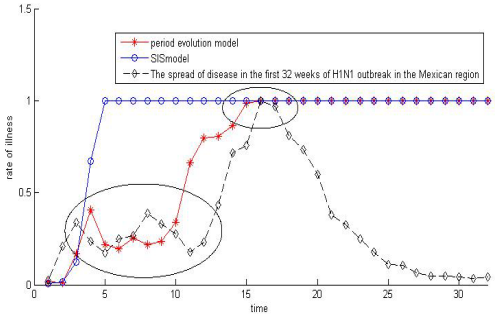

FIGURE 9. Virus propagation of two models compared to the real situation.

the evolution cycle leads to (18) becoming more accurate, resulting in a smaller gap between the model results and the actual data.

As Figure 9 shows, the model based on node evolution is closer to the real data. The proposed model can simulate the spread of the a virus given the results of pathological experiment and provide a more accurate prediction of actual virus spread. The model can be customized by setting different model coefficients to simulate different virus attacks and setting different initial values to reflect individual differences.

V. CONCLUSIONS

In this paper, viral propagation in a smart campus network was studied to improve the security and robustness of smart campuses. A new virus propagation model for the campus network applies a differential power system to describe a single network node; then, it uses graph theory and linear equations to link the evolution of each node with changes throughout the entire network. As is the case with a virus in an individual, the nodes in the smart campus network also have a certain degree of autonomy, which makes network research more complex. The improved model presented here can also be used to control both successive failures and public sentiment. In viral transmission, it can be found that under different immune initial values, autonomous individuals play a strong regulatory role. Therefore, regarding traffic congestion control and sequential failures, we can use this model to quantify the control strategy of each node into a single individual model, which can then be used to simulate and compare different control strategies to produce different effects on the smart campus network.

REFERENCES

[1] W. O. Kermack and A. G. McKendrick, "A contribution to the mathematical theory of epidemics," *Philos. Trans. Roy. Soc. London A, Math. Phys. Sci.*, vol. 115, no. 772, pp. 700–721, 1927.

[2] X. Y. He and X. F. Hu, "Dynamical modeling of information diffusion on Internet," *J. Syst. Simul.*, vol. 11, pp. 2511–2514, Oct. 2010.

[3] E. M. Sentovich *et al.*, "SIS: A system for sequential circuit synthesis," EECS Dept., Univ. California, Berkeley, Berkeley, CA, USA, Tech. Rep. UCB/ERL M92/41, May 1992.

[4] W. de Costa, L. Mediros, and S. Sandri, "A fuzzy cellular automata for SIR compartmental models," in *Fuzzy Logic and Applications* (Lecture Notes in Computer Science), vol. 8256. Nov. 2013, pp. 234–247.

[5] F. Nian and X. Wang, "Efficient immunization strategies on complex network," *J. Theor. Biol.*, vol. 264, pp. 77–83, May 2010.

[6] R. Parshai, S. Carmi, and S. Havlin, "Epidemic threshold for the susceptible-infectious-susceptible model on random networks," *Phys. Rev. Letter*, vol. 104, p. 258701, Jun. 2010.

[7] Q. G. Chen, "Research the dynamics behavior and immune control strategies of epidemic spreading on complex networks," *J. Southwest Univ.*, vol. 35, pp. 208–217, Jun. 2013.

[8] W. Wei *et al.*, "Gradient-driven parking navigation using a continuous information potential field based on wireless sensor network," *Inf. Sci.*, vol. 408, pp. 100–114, Oct. 2017.

[9] Y. Sun, H. Qiang, X. Mei, and Y. Teng, "Modified repetitive learning control with unidirectional control input for uncertain nonlinear systems," *Neural Comput. Appl.*, pp. 1–10, 2017, doi: 10.1007/s00521-017-2983-y.

[10] A. Yang *et al.*, "Optimum surface roughness prediction for titanium alloy by adopting response surface methodology," *Results Phys.*, vol. 7, pp. 1046–1050, Feb. 2017.

[11] K. Cui and X. Qin, "Virtual reality research of the dynamic characteristics of soft soil under metro vibration loads based on BP neural networks," *Neural Comput. Appl.*, vol. 29, no. 5, pp. 1233–1242, 2018, doi: 10.1007/s00521-017-2853-7.

[12] Y.-G. Sun, H.-Y. Qiang, J. Xu, and D.-S. Dong, "The nonlinear dynamics and anti-sway tracking control for offshore container crane on a mobile harbor," *J. Marine Sci. Technol.*, vol. 25, no. 6, pp. 656–665, Dec. 2012.

[13] Y. Zhao, X. M. Wang, and L. Li, "Virus spreading model on complex networks based on cellular automata," *Comput. Eng. Appl.*, vol. 51, pp. 117–122, Oct. 2015.

[14] T. Zhou *et al.*, "The opportunities and challenges of complex networks research," *J. Univ. Electron. Sci. Technol. China*, vol. 43, no. 1, pp. 1–5, Jan. 2014.

[15] R. Q. Li and W. Wang, "Review of threshold analysis about epidemic spreading dynamics on complex networks," *Complex Syst. Complex Sci.*, vol. 13, pp. 1–39, Oct. 2016.

[16] J. P. Gleeson, S. Mclink, and J. Ward, "Accuracy of mean-field theory for dynamics on real-world networks," *Phys. Rev. E, Stat. Phys. Plasmas Fluids Relat. Interdiscip. Top.*, vol. 85, p. 026106, Feb. 2012.

[17] S. R. Pastor and A. Vespignani, "Epidemic dynamics and endemic states in complex networks," *Phys. Rev. E, Stat. Phys. Plasmas Fluids Relat. Interdiscip. Top.*, vol. 63, p. 066117, May 2001.

[18] S. R. Pastor and A. Vespignani, "Epidemic dynamics in scale-free network," *Phys. Rev. E, Stat. Phys. Plasmas Fluids Relat. Interdiscip. Top.*, vol. 63, p. 066117, May 2001.

[19] Y. Moreno, R. Pastor-Satorras, and A. Vespignani, "Epidemic outbreaks in complex heterogeneous networks," *Eur. Phys. J. B-Condens. Matter Complex Syst.*, vol. 26, pp. 521–529, Apr. 2002.

[20] D. A. Rand, "Correlation equations and pair approximations for spatial ecologies," *Adv. Ecol. Theory, Principle Appl.*, vol. 12, pp. 329–368, Apr. 2009.

[21] J. P. Gleeson, "High-accuracy approximation of binary-state dynamics on networks," *Phys. Rev. Lett.*, vol. 107, p. 68701, Aug. 2011.

[22] N. Yang, "Study on the mechanism of influenza A (H1N1) virus-induced apoptosis of respiratory epithelial cells and the mechanism of PI4KB regulation of SARS coronavirus cells," Beijing Union Med. College, Beijing, China, Tech. Rep. 87, Oct. 2012.

[23] F. Liljeros, C. R. Edling, and L. A. N. Amaral, "The Web of human sexual contacts," *Nature*, vol. 411, pp. 907–908, May 2011.

[24] B. Bollobás and O. Riordan, "Coupling scale-free and classical random graphs," *Internet Math.*, vol. 1, pp. 215–225, Jan. 2004.

LEI WANG received the B.Sc., M.Sc., and Ph.D. degrees from the College of Communications Engineering, PLA University of Science and Technology, China, in 2006, 2010, and 2014, respectively. He is currently a Post-doctoral student and an Engineer in optimization and systems engineering. His research interests are optimization theory and multi-criteria decision making.

CHANGHUA YAO received the B.S. degree in automation from Zhejiang University in 2005 and the Ph.D. degree in communications and information systems from the PLA University of Science and Technology in 2016. He has been a Post-doctoral student with the Army Engineering University of PLA since 2017. His research interests include wireless networks, network security, opportunistic spectrum access, distributed optimization, data analysis, artificial intelligence, and machine learning.

YUQI YANG received the B.S. degree in automation from Zhejiang University in 2005 and the Ph.D. degree in communications and information systems from the PLA University of Science and Technology in 2016. He has been a Post-doctoral student with the Army Engineering University of PLA since 2017. His research interests include opportunistic spectrum access, distributed optimization, data analysis, artificial intelligence, and machine learning.

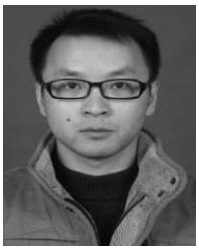

XIAOHAN YU received the Ph.D. degree in military operational research with the PLA University of Science and Technology in 2014. He is currently a Lecturer with the College of Command and Control Systems, Army Engineering University of PLA. He has authored over 30 scientific articles. His research interests include multi-criteria decision making, data mining, and military operations.